Propulsion and Power Research 2012;1(1):36–47

http://ppr.buaa.edu.cn/

Propulsion and Power Research

www.sciencedirect.com

ORIGINAL ARTICLE

An experimental investigation on the trailing edge cooling of turbine blades

Zifeng Yang, Hui Hu*

Department of Aerospace Engineering, Iowa State University, Ames, IA 50011, USA

Received 16 January 2012; accepted 11 September 2012
Available online 20 December 2012

KEYWORDS

Trailing edge cooling;
Wall slot jets;
Turbine blades;
Steroscopic particle image velocimetry (PIV) measurements;
Pressure sensitive paint (PSP) technique

Abstract An experimental study was conducted to quantify the flow characteristics of the wall jets pertinent to trailing edge cooling of turbine blades. A high-resolution stereoscopic particle image velocimetry (PIV) system was used to conduct detailed flow field measurements to quantitatively visualize the evolution of the unsteady vortices and turbulent flow structures in the cooling wall jet streams and to quantify the dynamic mixing process between the cooling jet stream and the mainstream flows. The detailed flow field measurements were correlated with the adiabatic cooling effectiveness maps measured by using pressure sensitive paint (PSP) technique to elucidate underlying physics in order to explore/optimize design paradigms for improved cooling effectiveness to protect the critical portions of turbine blades from harsh environments.

1. Introduction

Thermodynamic analysis reveals that thermal efficiency and power output of a gas turbine can be increased greatly with higher turbine inlet temperatures. Modern gas turbines are operating at a peak turbine inlet temperature well beyond the maximum endurable temperature of the turbine blade material. As a result, hot gas-contacting turbine blades have to be cooled intensively by using various techniques, such as internal convective cooling and film cooling on the blade exterior, in order to increase the fatigue lifetime of the turbine blades. One of the most

*Corresponding author.
E-mail address: huhui@iastate.edu (Hui Hu)

Peer review under responsibility of National Laboratory for Aeronautics and Astronautics, China.

Production and hosting by Elsevier

2212-540X © 2012 National Laboratory for Aeronautics and Astronautics. Production and hosting by Elsevier B.V. All rights reserved.
http://dx.doi.org/10.1016/j.jppr.2012.10.007

Nomenclature

H	height of the coolant slot
L	length of the upper plate of the trailing edge model
M	blowing ratio, $M=\rho U_{cooling}/\rho U_{main}$
Re_c	Reynolds number of the slot jet stream
TKE	turbulent kinetic energy, $TKE=\frac{1}{2U_\infty^2}\left(\overline{u'u'}+\overline{v'v'}+\overline{w'w'}\right)$
U_c	velocity of the cooling stream
U_∞	velocity of the mainstream flow
u, v, w	X, Y, Z component of the flow velocity
$\overline{u'}$, $\overline{v'}$, $\overline{w'}$	turbulent velocity fluctuations
X, Y, Z	Cartesian coordinate system
$\rho_{cooling}$	density of the cooling stream
ρ_{main}	density of the mainstream
η_{aw}	adiabatic cooling effectiveness
ω_z	vorticity in Z-direction

difficult regions to cool is the blade's trailing edges, due to geometric constraints in combination with aerodynamic demands. From an aerodynamic point of view the trailing edge should be designed as thin as possible in order to reduce aerodynamic losses. The demand usually conflicts with the blade structural integrity and cooling design requirements as coolant are not easily channeled into the thin trailing edges. It has been found that most of the catastrophic failures for turbine blades commonly originate at the edges–trailing edges, tips and roots. Common modes of failure are cracking, erosion, or simply melting. While trailing edge failure was found to greatly reduce the service time between maintenance, and severely restrict operating temperatures, surprisingly, only very few previous studies can be found in the open literature to address the thermal flow issues pertinent to trailing edge cooling of turbine blades. In this study, we particularly concern with the trailing edge cooling design of turbine blades.

The trailing edges of modern high pressure turbine blades are usually cooled by jets blown tangentially through a breakout slot on the pressure-side of the blade, which is shown schematically in Figure 1. Overheating is a consequence of failure of these cooling streams to protect the blade surface from hot free-stream gas. Sivasegaram and Whitelaw [1] evaluated the effects of lip thickness and injection angle of coolant streams on the cooling effectiveness for turbine blade film cooling. Denton [2] investigated the fundamental mechanism of aerodynamic loss pertinent to the trailing edge cooling design of turbine blades. At a basic level, the hot gas gets mixed to the surface, overheating the blades. Holloway et al. [3,4] found that trailing edge cooling is not as effective as anticipated: hot gas reaches the surface more readily than expected. For instance, numerical simulations based on steady, Reynolds-averaged analysis approaches predict notably better cooling effectiveness than the measured values obtained in the experiments done for blade design. More recently, numerical simulations of Medic and Durbin [5] have revealed that three-dimensional unsteadiness, which occurs in cooling slot jets, could be a primary cause of poor trailing edge protection. This suggests a potential path to re-designing the cooling streams to alleviate the heat load. While Medic and Durbin [5] showed that cooling jet streams contain unsteady, three-dimensional vertical components that have a large effect on transporting heat and contaminants to the surface due to the coherent, three-dimensional vortex shedding from the upper lip of the breakout slot, the computational evidence has not been verified yet experimentally.

While several experimental investigations have been conducted in recent years to investigate trailing edge cooling of turbine blades, the majority of those previous studies were conducted mainly based on the pressure loss measurements and the quantification of adiabatic cooling effectiveness on the wall downstream the breakout of cooling wall jet streams (see Taslim et al. [6], Brundage et al. [7], Cakan and Taslim [8] and Choi et al. [9]). Very few experimental studies (Martini et al. [10]) can be found in the literature to investigate the details of the flow characteristics of cooling wall jets in the cutback regions.

In the present study, an experimental investigation was conducted to quantify the flow characteristics of the wall jets pertinent to the trailing edge cooling of turbine blades. A high-resolution stereoscopic particle image velocimetry (SPIV) system was used to conduct detailed flow field measurements to quantitatively visualize the evolution of the unsteady vortex and turbulent flow structures in the cooling jet streams and to quantify the

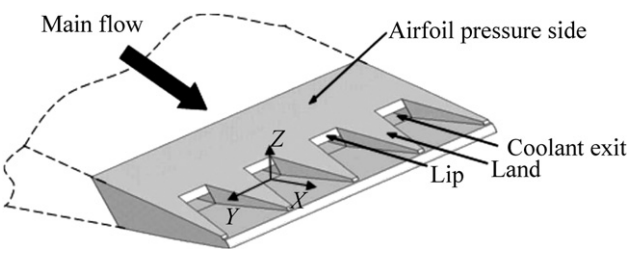

Figure 1 Trailing edge cooling slots at pressure side breakout.

dynamic mixing process between the cooling jet stream and the mainstream flows. Based on mass transfer analogy theory, pressure sensitive paint (PSP) was used to measure the adiabatic cooling effectiveness distribution on the protected surface in the cutback region of the trailing edge model. The detailed flow field measurements are correlated with the adiabatic cooling effectiveness measurements to elucidate underlying physics for improved understanding of the flow characteristics pertinent to trailing edge cooling of turbine blades. The findings derived from the present study can also be used to support the exploration of new trailing edge cooling strategies for improved cooling effectiveness to protect the critical portions of turbine blades from harsh environments.

2. Experimental setup

The experiments were conducted in a small open-circuit wind tunnel located at the Department of Aerospace Engineering of Iowa State University. The tunnel has a test section with an 8 inch × 5 inch (i.e., 200 mm × 125 mm) cross section. The walls of the test section are optically transparent. The tunnel has a contraction section upstream of the test section with honeycombs and screen structures installed ahead of the contraction section to provide uniform low-turbulence incoming flow into the test section. The turbulence intensity at the inlet of the test section was found to be less than 1.0% measured by using a hotwire manometer.

The test model used in the present study was designed to replicate only the trailing edge portion of a typical turbine blade. As shown schematically in Figure 2, the trailing edge of a turbine blade was simplified as a combination of two plates with six land structures to form five slot wall jets flowing tangentially along the surface of the lower plate. A relatively large plenum (a cubic box with 152 mm in length, width and height), which is mounted underneath the lower plate, was designed to settle the coolant flow (i.e., nitrogen). Two partition plates were mounted inside the plenum in order to maintain a uniform flow condition for the coolant stream before exhausted through the slot holes in the cutback region of the trailing edge model. Five long slot channels were engraved into the bottom side of the upper plate to let the coolant stream exhausted from the coolant plenum onto the cutback region of the trailing edge model as five slot wall jets. The turbulence intensity of the coolant stream at the exit of the slot holes was found to be about 7.0%, measured by using a hotwire anemometer.

In the present study, the lower surface of the trailing edge breakout model was coated with oxygen sensitive paint for the adiabatic film cooling effectiveness measurements by using PSP technique with mass transfer analogy [11–13]. While the airflow from the small wind tunnel was supplied to simulate the hot mainstream

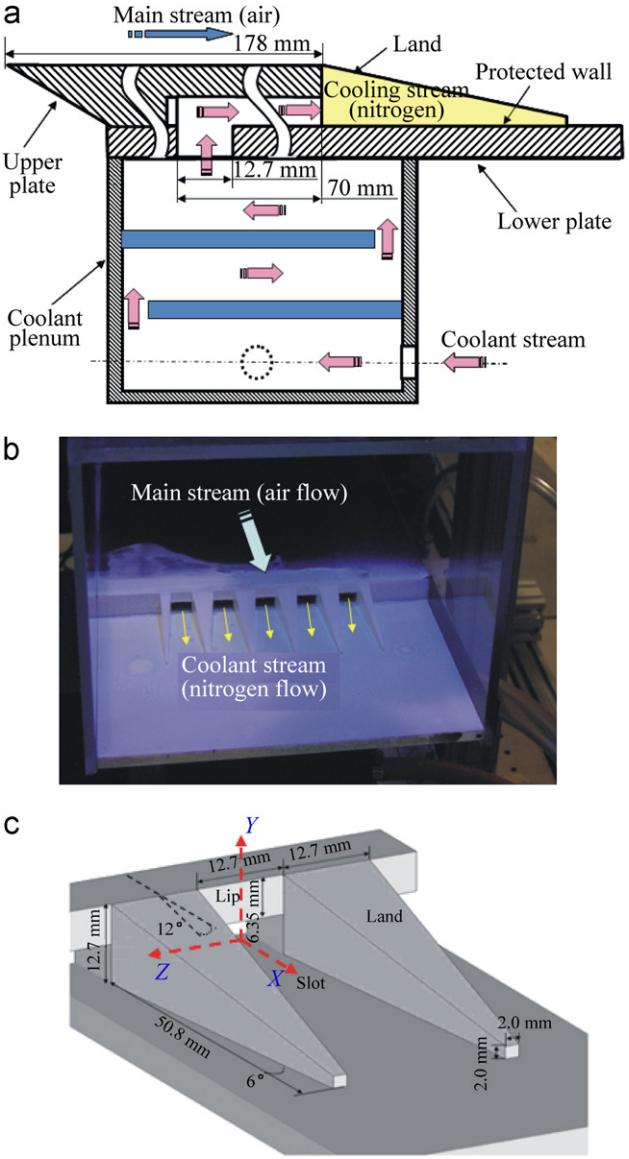

Figure 2 The trailing edge model used in the present study. (a) Side view of the trailing edge model, (b) a perspective view of the trailing edge model and (c) zoom-in view of the central slot channel.

flow, the cooling channel was fed by pure nitrogen to simulate the cooling jet stream to protect the surface on the lower plate. The mixing of the hot ambient gas into the cooling flow was simulated by the mixing of ambient airflow into the nitrogen jet stream.

During the experiments, the upper plate of the test model was flush mounted on the bottom wall of the test section. A 25 mm streamwise gap was held between the wind tunnel bottom wall and the sharp leading edge of the trailing edge model in order to remove the effects of the turbulent boundary layer from upstream. The main flow velocity at the inlet of the test section was set as $U_\infty = 16.2$ m/s. Based on the length of the trailing edge model, the corresponding Reynolds number was

3.15×10^5. The experimental study was conducted with five different blowing ratios, which is defined as the mass flux ratio between the cooling jet stream and mainstream, between 0 and 1.6. The corresponding Reynolds number of the cooling jet stream, Re_c is in the range of 0 to 11,000 based on the slot height H.

A high-resolution stereoscopic PIV system was in the present study to conduct detailed flow field measurements in the cutback region downstream the breakout slots of the trailing edge model. For the SPIV measurements, the mainstream airflow and the cooling nitrogen jet streams were seeded with ~1 μm oil droplets by using droplet generators. Illumination was provided by a double-pulsed Nd:YAG laser (NewWave Gemini 200) adjusted on the second harmonic and emitting two pulses of 200 mJ at the wavelength of 532 nm with a repetition rate of 10 Hz. The laser beam was shaped to a sheet by a set of mirrors, spherical and cylindrical lenses. The thickness of the laser sheet in the measurement region is about 1.0 mm. The illuminating laser sheet was first aligned along the main stream flow direction to conduct PIV measurements in the X–Y planes. Then, the laser sheet was rotated 90 degrees to illuminate flow structures in the cross planes normal to the main stream flow direction to conduct SPIV measurements in the Y–Z planes at different locations downstream of the slot exits.

For the stereoscopic PIV measurements in the Y–Z planes, two high resolution 14-bit CCD cameras (PCO1600, Cooke Corp.) were used for the SPIV image acquisitions. The two cameras were arranged in an angular displacement configuration to get a large overlapped view. With the installation of tilt-axis mounts, laser illumination plane, the lenses and camera bodies were adjusted to satisfy the Scheimpflug condition. The CCD cameras and the double-pulsed Nd:YAG lasers were connected to a workstation (host computer) via a Digital Delay Generator (Berkeley Nucleonics, Model 565), which controlled the timing of the laser illumination and the image acquisition. A general in-situ calibration procedure was conducted to obtain the mapping functions between the image planes and object planes for the stereoscopic PIV measurements. A target plate (~150 mm × 150 mm) with 500 μm-diameter dots spaced at intervals of 2 mm was used for the in-situ calibration. The mapping function used in the present study was a multi-dimensional polynomial function, which is fourth order for the directions parallel to the laser illumination plane (i.e., X and Y directions), and second order for the direction normal to the laser sheet plane (i.e., Z-direction). The coefficients of the multidimensional polynomial were determined from the calibration images by using a least-square method. For the PIV image processing, instantaneous PIV velocity vectors were obtained by a frame to frame cross-correlation technique involving successive frames of patterns of particle images in an interrogation window 32×32 pixels. An effective overlap of 50% of the interrogation windows was employed in SPIV image processing. For the SPIV measurements, with the mapping functions obtained by the in-situ calibration procedure, the two-dimensional displacements in the two image planes are used to reconstruct all three components of the velocity vectors in the laser illumination planes (i.e., Y–Z planes). After the instantaneous velocity vectors (u_i, v_i, w_i) were determined, instantaneous vorticity (ω_z) could be derived. The time-averaged quantities such as mean velocity (U, V, W), ensemble-averaged vorticity, turbulent velocity fluctuations ($\overline{u'}, \overline{v'}, \overline{w'}$) and normalized turbulent kinetic energy (TKE) distributions were obtained from a cinema sequence of 500 frames of instantaneous velocity fields.

In the present study, pressure sensitive paint (PSP) was used to measure the adiabatic film cooling effectiveness with the theory of the mass transfer analogy [9–13]. As shown in Figure 2(b), the surface of the lower plate was coated with Binary UniCoat oxygen sensitive paint. A UV light stroke at the wavelength of 400 nm was used to excite the sensor molecules pre-mixed in the oxygen sensitive paint. A CCD camera (PCO. 1600) with a 610 nm filter was used to acquire the photoluminescence image of the oxygen sensitive paint. During the experiments, the surface temperature of lower plate was also measured by using a thermocouple probe for the compensation of the temperature effects on the measurement results through a post-processing procedure. Further information about the SPIV and PSP techniques, experimental rig setup and test model, and measurement uncertainty analysis is available in Yang [14].

3. Results and discussions

3.1. PIV measurements in the centerline plane of the slot region of the cooling jet streams

PIV measurement results in the centerline plane of the slot region of the cooling jet streams were given in Figures 3 and 4 with the lands between the cooling slot jets removed. From the typical instantaneous velocity distribution at the blowing ratio of $M=0.43$ given in Figure 3, it can be seen clearly that the cooling jet stream would form a buffer layer between the protected surface on the lower plate and the mainstream flow until $X/H=4.0$ downstream (i.e., about 4 times of the slot height H, $H=6.35$ mm) of the breakout exit. A similar scenario was also found at the blowing ratios of 0.37 and 0.47 by Cakan and Taslim [8]. At further downstream, the cooling stream was found to mix with the mainstream flow intensively to generate a mixed turbulent boundary layer. Figure 3(b) shows the instantaneous vorticity distribution for the same conditions as described above. Compared with the vortex structures generated in a conventional 2-D mixing layer due to

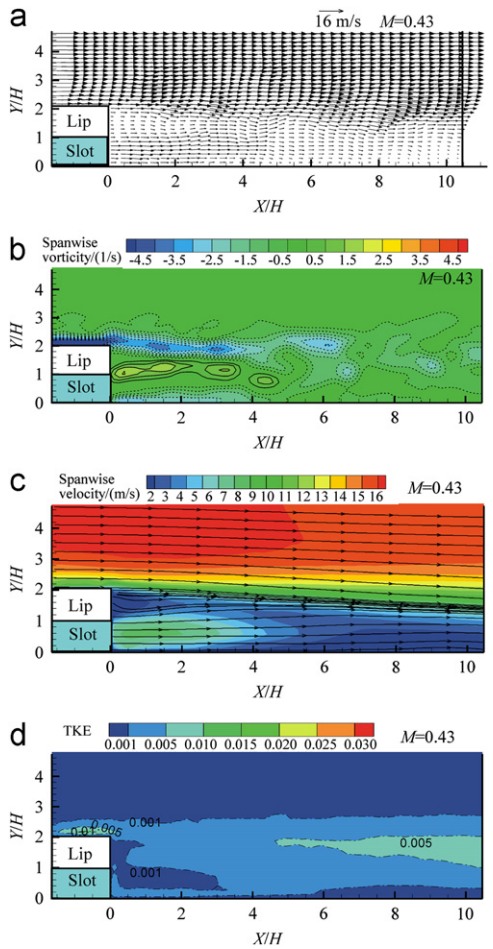

Figure 3 PIV results at the blowing ratio of $M=0.43$. (a) Instantaneous velocity vector field, (b) instantaneous vorticity contour, (c) averaged velocity with streamlines and (d) averaged turbulent kinetic energy.

Kelvin–Helmholtz instability, the vortex structures generated in the mixing layer between the cooling jet stream and mainstream flows were found to be much more complicated. This is observation is believed to be closely related to the three dimensionality of the slot jet flows. The ensemble-averaged flow velocity field shown in Figure 3(c) revealed clearly that the cooling jet stream exhausted from the slot exit would be able to form a buffer layer over the surface of the bottom wall in the region near to the slot exit before mixed with the mainstream flow intensively at further downstream. As shown clearly in the turbulent kinetic energy (TKE) distributions given in Figure 3(d), corresponding to the buffer layer over the protected bottom wall near the slot exit, a region with reasonably low TKE value was found in the near region of $X/H<3.0$. The TKE value was found to become much higher in the further downstream regions, which indicates that the mixing process between the cooling jet stream and mainstream flows would become much more intensive at downstream of $X/H>4.5$.

Figure 4 shows the PIV measurement results at the blowing ratio of $M=1.6$. As revealed clearly in the PIV measurements, at a high blowing ratio, the region at the downstream of the breakout exit would be filled with high-speed cooling stream flow, which will expel the mainstream flow away from the protected surface in the cutback region. The instantaneous vorticity field and averaged TKE distribution reveal clearly that the buffer layer formed by the cooling stream in the region between the mainstream flow and the protected surface would be extended to much further downstream (i.e., $X/H>8.0$). It can also be seen clearly that, due to the entrainment of the higher momentum of the cooling stream at a high blowing ratio, the intensive mixing between the cooling stream and the mainstream flow would lead to the invasion of the mainstream flow into the region near the surface of the protected wall, as revealed clearly in the ensemble-averaged velocity distribution as the streamlines of the mainstream tilting more towards the protected wall at the upper boundary

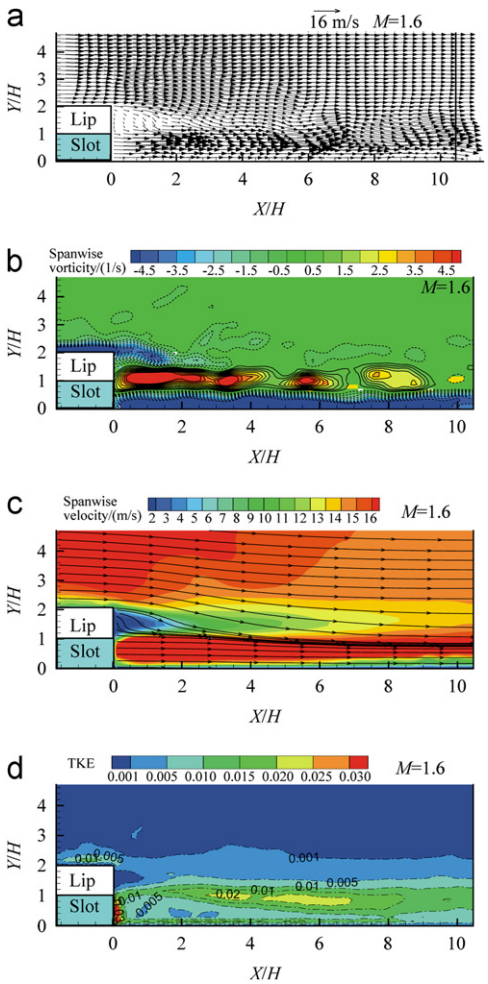

Figure 4 PIV results at the blowing ratio of $M=1.6$. (a) Instantaneous velocity vector field, (b) instantaneous vorticity contour, (c) averaged velocity with streamlines and (d) averaged turbulent kinetic energy.

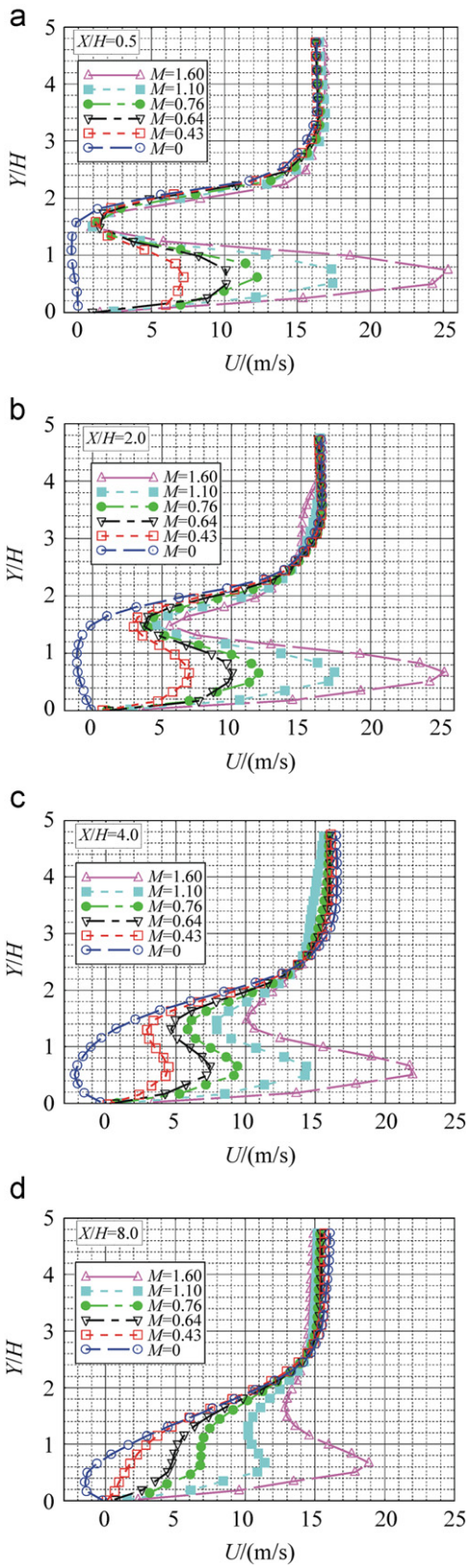

Figure 5 Velocity profiles at different downstream locations. (a) $X/H=0.5$, (b) $X/H=2.0$, (c) $X/H=4.0$ and (d) $X/H=8.0$.

of the buffer layer. Such flow pattern is quite different from the observations for the cases at low blowing ratios. For example, as shown clearly in Figure 3, the streamlines of the cooling stream would be lift upward in the region of $X/H<4.0$ at the low blowing ratio of $M=0.43$ due to the entrainment of the higher momentum of the mainstream flows. It can also be seen clearly that the downward slope of the streamlines of the mainstream flow at the downstream of the breakout exit would become much larger for the case with high blowing ratio case of $M=1.60$ compared with the one with low blowing ratio of $M=0.43$.

Figure 5 shows the transverse velocity profiles of the streamwise velocity as a function of the downstream distance away from the breakout exit at different blowing ratios. It can be seen clearly that, for the case without cooling stream exhausted from the cooling slot exit, i.e., the case with the blowing ratio of $M=0$, the streamwise velocity in the near wall region (i.e., $Y/H<2.0$) at the downstream of the breakout exit was found to be negative. It indicates that a recirculation region will be generated in the downstream of the cutback region of the trailing edge model, as expected. For all the other cases, the transverse profiles were found not to vary too much in the near wall region as the downstream distance increasing from $X/H=0.5$ to $X/H=2.0$. It indicates that the mixing between the slot cooling jet stream and the mainstream flow would be limited in the region near the breakout exit. As the downstream distance increasing, the difference of the streamwise velocity in the cooling jet stream (i.e., $Y/H=0$–1) and the mixing region (i.e., $Y/H=1$–2) was found to decrease rapidly due to the intensive mixing between the cooling stream and the mainstream flows. For the case at blowing ratio of $M=0.43$, the difference of the streamwise velocity in the cooling slot stream (i.e., $Y/H=0$–1) and the mixing region (i.e., $Y/H=1$–2) was found to be less than 1.5 m/s at the downstream location of $X/H=4.0$. As the downstream distance reaching $X/H=8.0$, the transverse velocity profiles were found to become monotonically increased curves for all the cases with the blowing ratios less than 1.0 (i.e., $M<1.0$). It would indicate an almost completely mixing between cooling stream and the mainstream flows. It would also suggest that the cooling stream will not be able to effectively protect the surface of the bottom plate from the invasion of the mainstream flow any more at the further downstream locations, which was confirmed quantitatively from the cooling effectiveness measurements shown in Figure 12.

It should be noted that the measurement results given in the present study were obtained with a density ratio of the cooling stream and mainstream being about 1.0, which is much smaller compared with the density ratio

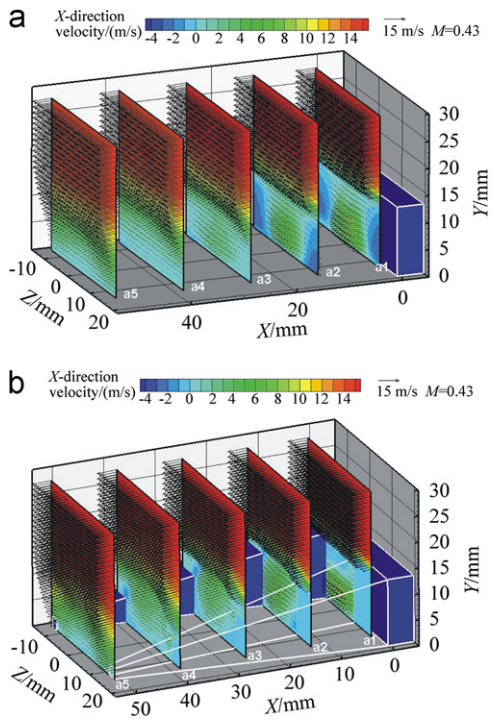

Figure 6 Stereoscopic PIV results at the blowing ratio of $M=0.43$, (a) without land and (b) with land.

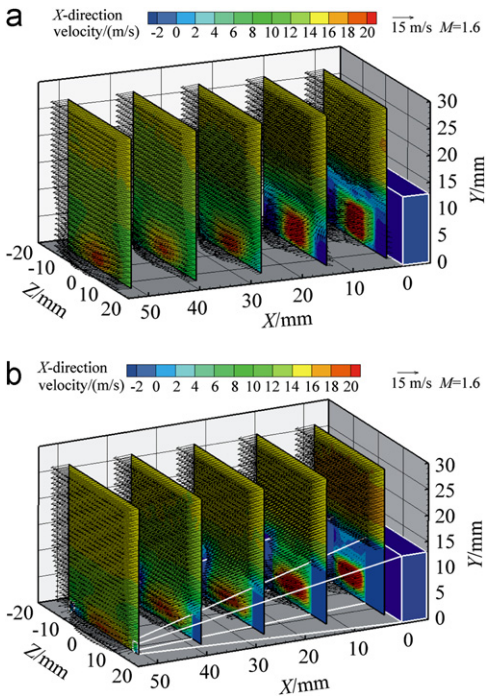

Figure 7 Stereoscopic PIV results at the blowing ratio of $M=1.6$, (a) without land and (b) with land.

values of real engine applications (i.e., about 1.5 for of real engine applications). A comprehensive study is planned to assess the effects of the density ratio of the cooling streams to the mainstream flows on the flow characteristics of the mixing process between the cooling streams and mainstream flows as well as the effectiveness of trailing edge cooling design of turbine blades.

3.2. Stereoscopic PIV measurement results at different downstream locations

3.2.1. The effects of the blowing ratios

Figure 6 shows the three-dimensional flow velocity vectors and the contours of the streamwise velocity values for the test cases without and with lands mounted in the breakout region at the blowing ratio of $M=0.43$. The measurement planes, a1 to a5, were located at $X/H=1.0$, 2.0, 4.0, 6.0 and 8.0 downstream of the breakout exit. It can be seen clearly that the cooling streams exhausted from the breakout exit would have a jet shaped flow feature near the slot exit, as expected. As shown in Figure 6, the jet shaped flow feature was found to become almost distinguishable in the further downstream, e. g., in the last two cross planes of a4 and a5, which indicates an almost complete mixing between the cooling stream and the mainstream flows. For the case without lands, inverse flows were found at two sides of the slot exit as revealed clearly in the measurement planes of a1 and a2 shown in Figure 6(a). This is because 'recirculation' zones would be formed in the regions between the two neighboring cooling slot jets, as one might expect. As shown in Figure 6(b), the inverse flows would be eliminated as the lands were mounted in the cutback region of the trailing edge model.

Figure 7 shows the three-dimensional flow velocity vectors and the contours of the streamwise velocity values at the blowing ratio of $M=1.6$. The jet shaped cooling stream was revealed more clearly compared with the cases at relatively low blowing ratios. The jet shape feature of the cooling stream was found to be preserved very well all the way up to the farthest boundary of the measurement region (i.e., up to downstream locations of $X/H>8.0$). The better preserved jet shape of the cooling stream at higher blowing ratios would indicate a better coverage of the cooling stream over the protected surface, i.e., better cooling effectiveness. The regions with high-speed cooling jet stream were found to be wider for the case with the lands compared with those without the lands. It indicates that the existence of lands would be beneficial to guide the cooling streams to protect the surface of the bottom plate at the downstream of the breakout exit.

The distributions of the streamwise vorticity of the mixing flow in the cutback region of the trailing edge model can be derived based on the stereoscopic PIV measurement results. Figure 8 shows the ensemble-averaged vorticity distributions in three typical cross planes for the test cases with the blowing ratio $M=0.43$ and $M=1.60$. Streamwise vortices in a mixing flow have

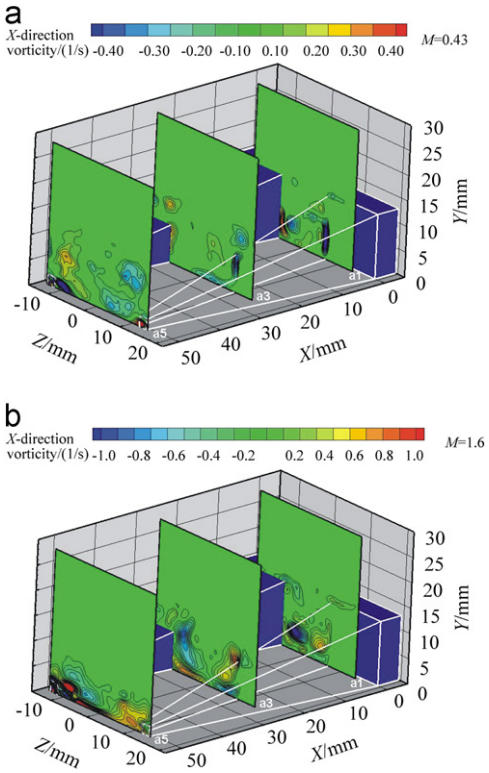

Figure 8 Averaged streamwise vorticity contour with varied blowing ratios for the cases with lands, (a) $M=0.43$ and (b) $M=1.60$.

been suggested to play a very important role to enhance the mixing process [12]. As shown clearly in Figure 8, several streamwise vortices with adverse signs in the streamwise vorticity distributions (i.e., an adverse rotational direction) can be identified in the measured cross planes. The streamwise vortices were found to be much stronger in the cross-planes at further downstream locations, corresponding to more intensive mixing between the cooling stream and the mainstream flows. The measurement results also revealed clearly that streamwise vortex structures could originate from the upper lips of the breakout exits, which agrees with the findings reported by Medic and Durbin [5]. For the cases with relatively low blowing ratios (i.e., $M<1.0$), the entrainment of the high momentum mainstream flow would cause the cooling stream to escape from the slot channel around the ridges of the lands, which resulted in the generation of the streamwise vortices sitting on the ridges of the lands. As shown in Figure 8(b), the streamiwse vortices were found to be concentrated at the bottom corners of the channel as the blowing ratio becomes relatively high. In conclusion, the blowing ratio was found to have significant effects on the formation of the streamwise vortex structures at the downstream of the breakout exit.

3.2.2. *The effects of the existence of the lands*

Figures 9 and 10 show the ensemble-averaged SPIV measurement results in the cross planes at different downstream locations for the cases with and without the lands mounted in the breakout region at the blowing ratio $M=0.43$ and $M=1.60$. The effects of the existence of the lands on the mixing process between the cooling streams and the mainstream flows were revealed clearly from the comparisons of the measurement results. As shown in Figures 9 and 10, for the cases without the lands, the cooling streams were found to expend laterally (i.e., along Z-direction) after exhausted from the breakout exit, as indicated by the large lateral component (i.e., Z-component) of the velocity vectors for the SPIV measurement results in the $X/H=2.0$ cross plane. As a result, the cooling streams would also be able to cover the surface of the regions between the neighboring slot cooling jets, in addition to the region at the downstream of the breakout exits. The lateral expansion of the cooling stream was found to decay rapidly as the downstream distance increases due to the intensive mixing between the cooling stream and the mainstream flows at further downstream, as revealed from the SPIV measurement results in the $Z/H=4.0$ and $Z/H=8.0$ cross planes.

For the case with the lands mounted in the cutback of the trailing edge model, a slot channel would be formed at the downstream of each breakout exit due to the existence of the lands. The cooling stream exhausted from the breakout exit would be guided by the lands to flow smoothly over the protected surface inside the slot channel. However, the lateral expansion of the cooling stream would be restricted due to the existence of the lands, as indicated by the much smaller lateral component (i.e., Z-component) of the velocity vectors revealed from the SPIV measurements. As a result, the cooling stream would more readily flow inside the slot channel to protect the surface inside the slot channel between the neighboring lands. It can also be seen clearly that, at the same downstream locations, the invasion of the mainstream flow to the near wall region was found to be much less for the case with the lands compared with that without the lands. It indicates that the existence of the lands would be beneficial to improve the coverage of the cooling stream over the surface of the cutback region along the flow direction, while the lateral expansion of the cooling stream will be restricted by the existence of the lands at the downstream of the breakout exits.

Based on the stereoscopic PIV measurements as shown in Figures 9 and 10, the schematics of the streamlines and vortex structures in the cutback region were derived, which were shown in Figure 11. As described above, a series of streamwise vortices would be generated at the corners of the slot channel, which are closely related to the mixing process of the cooling streams with the mainstream flows in the cutback region. For the cases with the blowing ratio smaller than 1.0 (i.e., $M<1.0$), the cooling stream would be entrained by the high-momentum mainstream flows. When viewing from upstream along the streamlines of the cooling streams, the streamwise vortices at the left corners of the slot channel were found to be counterclockwise, while the

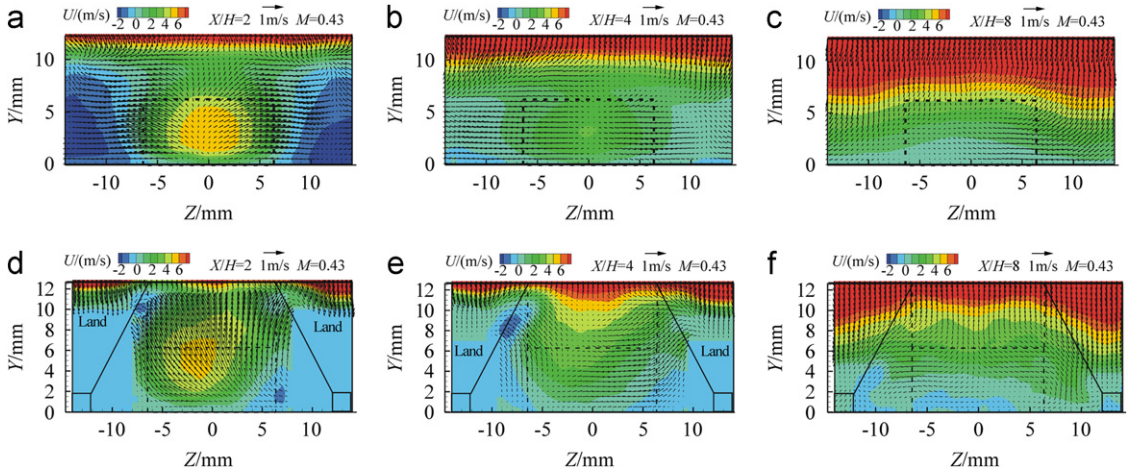

Figure 9 Stereoscopic PIV measurement results in three typical cross planes with the blowing ratio $M=0.43$, (a) at $X/H=2.0$ without the lands, (b) at $X/H=4.0$ without the lands, (c) at $X/H=8.0$ without the lands, (d) at $X/H=2.0$ with the lands, (e) at $X/H=4.0$ with the lands and (f) at $X/H=8.0$ with the lands.

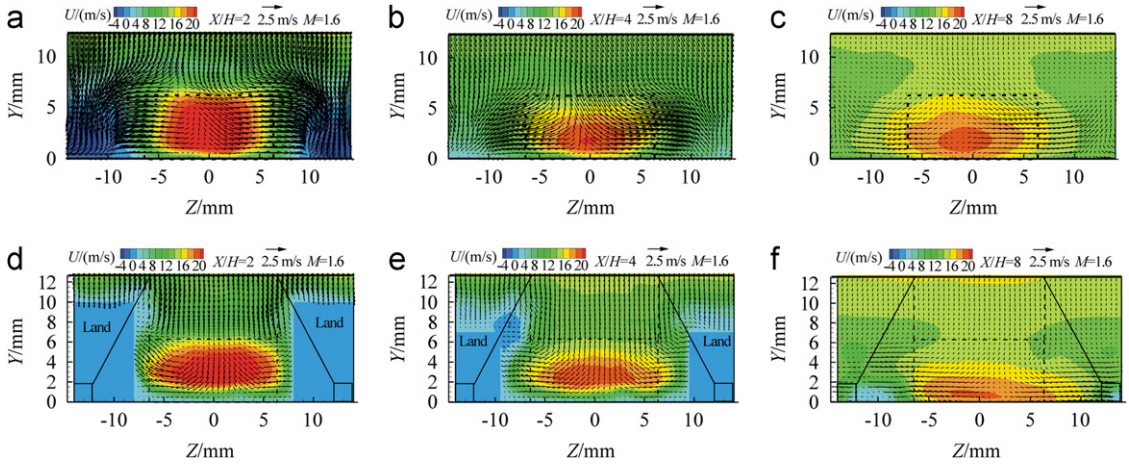

Figure 10 Stereoscopic PIV measurement results in three typical cross planes with the blowing ratio $M=1.60$, (a) at $X/H=2.0$ without the lands, (b) at $X/H=4.0$ without the lands, (c) at $X/H=8.0$ without the lands, (d) at $X/H=2.0$ with the lands, (e) at $X/H=4.0$ with the lands and (f) at $X/H=8.0$ with the lands.

vortices at the right corners of the slot channel were clockwise. As a result, the streamwise vortices would promote the cooling stream climbing up around the ridges of the lands to cover the top surfaces of the lands, which would contribute to the relatively good film cooling effectiveness on the top surfaces of the lands at relatively low blowing ratios as confirmed from the PSP measurements shown in Figure 12. Conversely, as the blowing ratio becomes greater than 1.0, the mainstream flow would be entrained by the high-momentum cooling streams. After exhausted from the breakout exit, the high-momentum cooling stream would more readily flow along the slot channels and provide a better protection over the bottom surfaces of the slot channels, which results in almost perfect film cooling effectiveness on the surfaces inside the slot channels, which was also revealed quantitatively from the PSP measurements given in Figure 12. The streamwise vortices at the corners of the slot channel were found to reverse their direction with the clockwise vortices at the left corners and counterclockwise vortices at the right corners of the slot channels as the blowing ratio becomes greater than 1.0. The streamwise vortices would limit the climbing up of the cooling streams to cover the top surfaces of the lands. It would result in the relative low film cooling effectiveness on the top surfaces of the lands, as confirmed from the PSP measurement results shown in Figure 12. Since the cooling streams with higher momentum would more readily flow inside the slot channels as the blowing ratio increases, the film cooling effectiveness on the tops of the lands was found to become lower and lower. Similar phenomena were also revealed by the numerical simulations of Chen et al. [15].

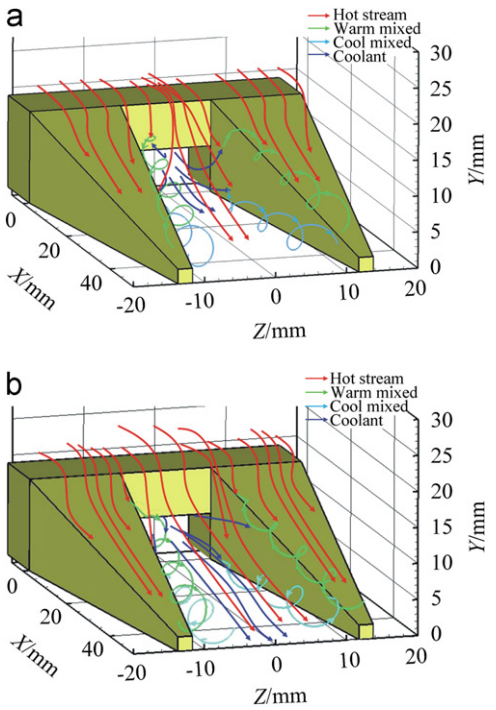

Figure 11 Schematic of the flow structures in the cutback region, (a) at low blowing ratio and (b) at high blowing ratio.

3.3. PSP measurement results

As aforementioned, pressure sensitive paint (PSP) technique was used in the present study to measure the adiabatic film cooling effectiveness with the theory of the mass transfer analogy [9–13]. Figure 12 shows some typical PSP measurement results in the term of adiabatic cooling effectiveness distributions on the protected surface in the cutback region at different blowing ratios. It can be seen clearly that, since the cooling streams were exhausted from the breakout slots, the regions with relatively high cooling effectiveness were found to concentrate near to the breakout exit, the regions on the top surfaces of the lands were found to have relatively low cooling effectiveness, as expected. It should be noted that, since there is no PSP paint applied in the regions upstream of the breakout exits (i.e., the regions of $X/H<0.0$), the cooling effectiveness in the regions was set to be zero during the PSP image processing.

As the blowing ratio increases, the cooling effectiveness over the protected surface inside the slot channels was found to become higher and higher since more cooling streams would be exhausted from the breakout exits to cover the protected surfaces. As shown in Figure 12, the best adiabatic cooling effectiveness was found to be achieved at the highest blowing ratio of $M=1.6$ for the present study, as expected. It should be noted that the cooling effectiveness distribution at $M=1.1$ shows a slightly different trend for the regions close to the ends of the lands compared with all the other cases. Such characteristic distribution was also observed by Joo and Durbin [16] in their large eddy simulations. Such result is also believed to be closely related to the findings suggested by Holloway [3–4] that the effects of the vortex shedding on the mixing process of the cooling streams and mainstream flows is most intensive for the blowing ratios around unity. The intensive mixing between the cooling streams and the mainstream flows in the regions near the channel centerline as well as the relatively weak mixing in the regions near lands may be responsible for the pattern revealed from the adiabatic cooling effectiveness distribution at the blowing ratio of $M=1.1$.

It should also be noted that the adiabatic cooling effectiveness on top surfaces of the lands was found to decrease drastically as the blowing ratio increases. This can be explained by the different characteristics of the vortex structures in the cutback region at different blowing ratios, as shown in Figure 11. For the cases with relatively low blowing ratios ($M<1.0$), the cooling stream inside the slot channel would tend to climb up around the ridges of the lands due to the entrainment of the high-momentum mainstream flows. The rotation direction of the streamwise vortices generated at the corners of the slot channel would be helpful to pump more cooling stream to climb up around the ridges of the lands to reach to the top surfaces of the lands. As a result, it would be easier for the cooling streams to create more coverage in the lateral direction and provide a relatively good protection on the top surfaces of the lands. However, for the cases with relatively high blowing ratios ($M>1.0$), the mainstream flows would be entrained by the high-momentum cooling streams, which resulted in a downward flow pattern of the mainstream flow in the region near the centerline of the slot channel as shown in Figure 10. The cooling streams exhausted from the breakout exit would readily flow along the slot channels between the lands rather than expand laterally to reach to the top surfaces of the lands. The streamwise vortices generated at the corners of the slot channels were also found to reverse their rotation direction compared with those at relatively low blowing ratios, which would restrict the cooling streams inside the slot channels. As a result, the adiabatic cooling effectiveness on the top surfaces of the lands was found to decrease drastically as the blowing ratio increases. The similar finding was also reported by Chen et al. [15], whose numerical simulation revealed very high cooling effectiveness inside the cutback slots with almost no heat flux across the slot channels for the cases with relatively high blowing ratios (i.e., $M>1.3$).

4. Concluding remarks

An experimental study was conducted to investigate the evolutions of the turbulent flow and vortex structures in the slot wall jets pertinent to the trailing edge cooling of turbine blades. A stereoscopic PIV system was used to conduct detailed flow field measurements of the slot wall jet flows

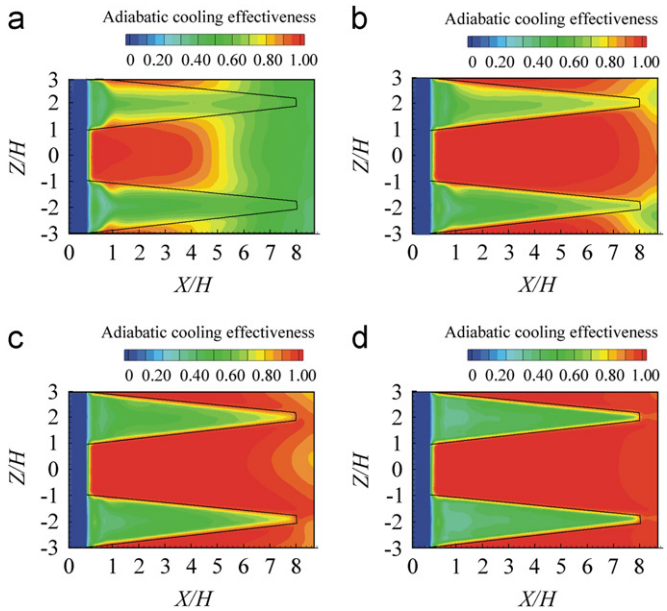

Figure 12 Adiabatic cooling effectiveness on the trailing edge for different blowing ratios, (a) $M=0.43$, (b) $M=0.80$, (c) $M=1.10$ and (d) $M=1.60$.

exhausted from the breakout exits of a typical trailing edge model of gas turbine blades. Pressure sensitive paint (PSP) technique was used to measure the adiabatic cooling effectiveness distributions over the protected surface in the breakout region of the turbine blade trailing edge model. The effects of the blowing ratio of the cooling streams on the flow mixing between the mainstream flows and cooling jet streams and the resultant adiabatic film cooling effectiveness distributions over the protected surfaces were investigated in great detail. The detailed flow field measurements are correlated with the adiabatic cooling effectiveness measurements to elucidate underlying physics for improved understanding of the flow characteristics pertinent to trailing edge cooling of turbine blades. The findings derived from the present study can also be used to support the exploration of new trailing edge cooling strategies for improved cooling effectiveness to protect the critical portions of turbine blades from harsh environments.

Acknowledgments

The authors are grateful to Dr. Tom IP Shih of Purdue University for technical discussions, and Mr. Bill Rickard and Anand Goppa Kumar of Iowa State University for their help in conducting the experiments. The support of the National Science Foundation CAREER Program under Award no. of CTS-0545918 is gratefully acknowledged.

References

[1] S. Sivasegaram, J.H. Whitelaw, Film cooling slots: the importance of lip thickness and injection angle, Journal of Mechanical Engineering Science 11 (1) (1969) 22–27.

[2] J.D. Denton, The 1993 IGTI Scholar lecture: loss mechanisms in turbomachines, ASME Journal of Turbomachinery 115 (4) (1993) 621–656.

[3] S.D. Holloway, J.H. Leylek, F.A. Buck, Pressure-side bleed film cooling, part 1: steady framework for experimental and computational results, ASME Paper no. GT-2002-30471, 2002.

[4] S.D. Holloway, J.H. Leylek, F.A. Buck, Pressure-side bleed film cooling, part 2: unsteady framework for experimental and computational results, ASME Paper no. GT-2002-30472, 2002.

[5] G. Medic, P.A. Durbin, Unsteady effects on trailing edge cooling, ASME Journal of Heat Transfer 127 (2005) 388–392.

[6] M.E. Taslim, S.D. Spring, B.P. Mehlman, An experimental investigation of film cooling effectiveness for slots of various exit geometries, Journal of Thermophysics and Heat Transfer 6 (2) (1992) 302–307.

[7] A.L. Brundage, M.W. Plesniak, P.B. Lawless, S. Ramadhyani, Experimental investigation of airfoil trailing edge heat transfer and aerodynamic losses, Experimental Thermal and Fluid Secience 31 (2007) 249–260.

[8] M. Cakan, M.E. Taslim, Experimental and numerical study of mass/heat transfer on an airfoil trailing-edge slots and lands, ASME Journal of Turbomachinery 129 (2007) 281–293.

[9] J.H. Choi, S. Mhetras, J.C. Han, S.C. Lau, R. Rudolph, Film cooling and heat transfer on two cutback trailing edge models with internal perforated blockages, ASME Journal of Heat Transfer (2008), http://dx.doi.org/10.1115/1.2780174 012201.1–13.

[10] P. Martini, A. Schulz, H.-J. Bauer, Film cooling effectiveness and heat transfer on the trailing edge cutback of gas trubine airfoils with vairous internal cooling designs, ASME Journal of Turbomachinery 128 (1) (2006) 196–205.

[11] J. Ahn, S. Mhetras, K.C. Ha, Film-cooling effectiveness on a gas turbine blade tip using pressure-sensitive paint, ASME Journal of Heat Transfer 127 (5) (2005) 521–530.

[12] A. Suryanarayanan, S.P. Mhetras, M.T. Schobeiri, J.C. Han, Film-cooling effectiveness on a rotating blade platform, ASME Journal of Turbomachinery 131 (1) (2009), http://dx.doi.org/10.1115/1.2752184 011014.1–12.
[13] Z. Yang, H. Hu, Trailing edge cooling effectiveness measurements of turbine blades using pressure sensitive paint (PSP) technique, AIAA Journal of Propulsion and Power 27 (3) (2011) 700–709.
[14] Z. Yang, Experimental investigations on complex vortex flows using advanced flow diagnostic techniques, Ph.D. Dissertation, Iowa State University, Iowa, 2009.
[15] S.P. Chen, P.W. Li, M.K. Chyu, F.J. Cunha, W. Abdel-Messeh, Heat transfer in an airfoil trailing edge configuration with shaped pedestals mounted internal cooling channel and pressure side cutback, ASME Paper no. GT2006-91019, 2006.
[16] J. Joo, P.A. Durbin, Simulation of turbine blade trailing edge cooling, ASME Journal of Fluids Engineering 131 (2) (2009) 021102.1-14.